

RESEARCH

Open Access



Ultrasound-activated nano-TiO₂ loaded with temozolomide paves the way for resection of chemoresistant glioblastoma multiforme

Fawad Ur Rehman^{1*†}, Mohd Ahmar Rauf^{2†}, Sajjad Ullah³, Sana Shaikh⁴, Aqsa Qambrani⁴,
Pir Muhammad^{1*} and Sumaira Hanif¹

*Correspondence:
fawad@henu.edu.cn;
pir@henu.edu.cn

[†]Fawad Ur Rehman
and Mohd Ahmar Rauf
contributed equally

¹ International Joint Centre
for Biomedical Innovations,
School of Life Sciences,
Henan University, Jin Ming
Avenue, Kaifeng 475004,
Henan, China

Full list of author information
is available at the end of the
article

Abstract

Background: Glioblastoma multiforme (GBM) is one of the most daunting issues to modern therapeutics, with a higher mortality rate post-diagnosis. Temozolomide (TMZ) is the only available treatment; however, the frequent resistance leaves the oncologists at a dead end. Therefore, new approaches to circumvent the GBM are highly desired. We have employed TiO₂ nanosticks loaded with TMZ as nanomedicine for TMZ-resistant GBM resection in this contribution.

Results: The ultrasonication triple-action effect could greatly facilitate tumor ablation by enhancing the TiO₂ nanosticks traversing across BBB, releasing the TMZ payload from TiO₂ nanosticks and reactive oxygen species (ROS) generation from TiO₂ nanosticks within the GBM milieu. The tumor ablation was confirmed by MTT and Annexin(v)-PI assays, apoptotic proteins expression via western blot and ROS level detection in vitro, whereas tumor volume, weight, survival rate, and relative photon flux in the xenograft and orthoptic TMZ-resistant GBM murine models as in vivo.

Conclusion: We found this nanomedicine-based ultrasound modality highly efficient in GBM treatment and is of future clinical application value due to the employment of already FDA-approved techniques and nanomedicine.

Keyword: Temozolomide resistance, Glioblastoma multiforme, Ultrasound, TiO₂ nanosticks, Blood–brain barrier

Background

Glioblastoma is a major glioma that primarily affects the central nervous system and is known with highly engraved prognosis and post-diagnosis patient survival for less than 15 months (Xu et al. 2017; Patel et al. 2019). Temozolomide (TMZ) is the only Food and Drug Administration (FDA) approved therapeutic agent for GBM that could merely add several months to the survival of patients and is mainly used as adjuvant therapy after surgical resection of the tumor (Chamberlain 2010). In addition, the suboptimal concentration of TMZ at the tumor site, frequent development of chemoresistance, and the



© The Author(s) 2021. This article is licensed under a Creative Commons Attribution 4.0 International License, which permits use, sharing, adaptation, distribution and reproduction in any medium or format, as long as you give appropriate credit to the original author(s) and the source, provide a link to the Creative Commons licence, and indicate if changes were made. The images or other third party material in this article are included in the article's Creative Commons licence, unless indicated otherwise in a credit line to the material. If material is not included in the article's Creative Commons licence and your intended use is not permitted by statutory regulation or exceeds the permitted use, you will need to obtain permission directly from the copyright holder. To view a copy of this licence, visit <http://creativecommons.org/licenses/by/4.0/>. The Creative Commons Public Domain Dedication waiver (<http://creativecommons.org/publicdomain/zero/1.0/>) applies to the data made available in this article, unless otherwise stated in a credit line to the data.

blood–brain barrier (BBB) selective amenability are some of the major bottlenecks in complete resection of GBM (Haar et al. 2012; Casals et al. 2017; Bahadur et al. 2019).

The BBB is a physiological barrier comprising endothelial cells having tight junctions, basal membrane, and podocytes of astrocytes (Pardridge 2007). The primary mandate of BBB is the central nervous system homeostasis and protection against potentially toxic substances. The BBB is only amenable to small molecules (i.e., < 400 Da size and < 9 hydrogen bonding, CO₂, O₂, alcohol, and glucose, etc.) (Abbott et al. 2006). It constrains 98% of all other biochemicals and drugs that may be efficient therapeutic agents in other parts of the body (Mitragotri 2013). Therefore, modalities that increase the BBB amenability for the cure of CNS ailments are highly valued. For instance, the focused ultrasound has been reported to open the BBB via micro/nanobubbles formation (Bing et al. 2018; Wu et al. 2018) and allow maximum drug accumulation in the brain. Recently, Liu et al. (2014) employed focused ultrasound to reversibly break the BBB and enhance the TMZ localization in GBM from 6.98 to 19 ng/mg. Likewise, during the phase I clinical trial, Lipsman et al. (2018) employed focused ultrasound to open BBB in Alzheimer's disease (AD) patients, consequently lowering the β amyloid plaques and tau protein aggregates resulting in AD's amelioration.

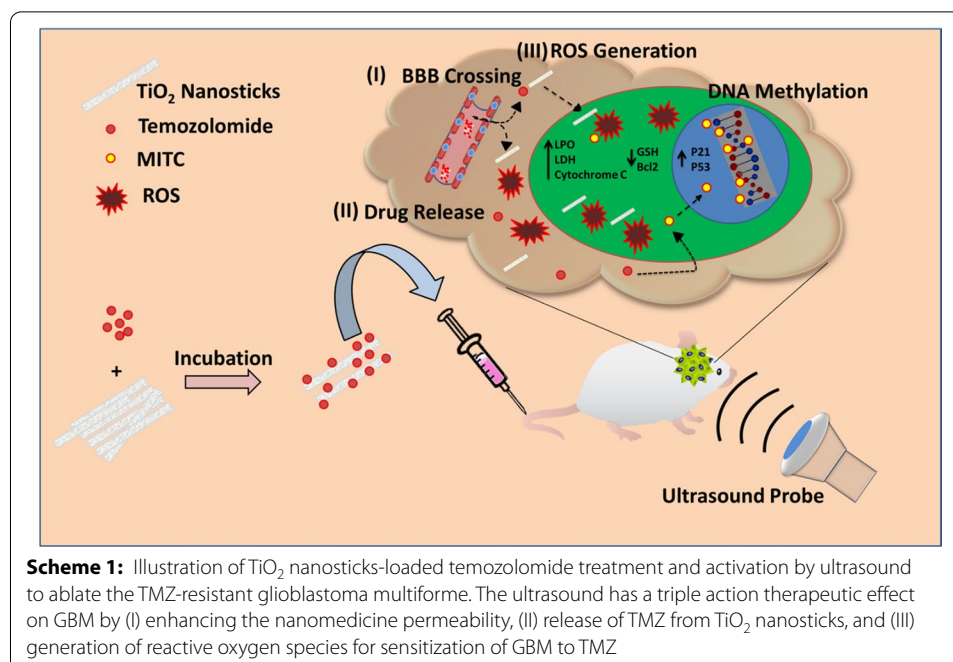
The nanotechnology-based approaches have also been more efficient in drug delivery to targeted tissues (viz brain) than free drugs (Srikanth and Kessler 2012; Mi et al. 2016; Rehman 2020; Younas Iqbal et al. 2020). For instance, nanoscale TiO₂ has been reported with promising biomedical applications and higher biocompatibility that has already been recognized by FDA (Rehman et al. 2016a, b; Youssef et al. 2017). The TiO₂ nanosticks provide a large surface area and efficient scaffold for drug delivery due to their porous nature. Moreover, upon excitation with ultrasound waves, the nanoscale TiO₂ can produce reactive oxygen species (ROS), including OH, H₂O₂, HO₂, ¹O₂, and O₂ can efficiently induce apoptosis in the tumor by interfering with cellular signaling pathways (Zhao et al. 2015). Recently, Harada et al. (2013) reported that nanoscale TiO₂ could generate the singlet oxygen (¹O₂) within HeLa cells and thus exert cytotoxic effects leading to apoptosis. Similarly, Deepagan et al. (2016) used Au–TiO₂ nanocomposites to ablate tumors via sonodynamic therapy. In contrast, Ninomiya et al. (2014) used only TiO₂ nanoparticles to arrest the growth of the HepG2 cells by 46% after sonication.

To establish a robust nano-drug delivery system that could efficiently deliver the therapeutic cargo to GBM across the BBB and resect the TMZ-resistant GBM, we established the TiO₂ nanosticks-based drug delivery system for TMZ delivery to GBM. Moreover, the ultrasound triple-action trigger could open the BBB and further added to the release of TMZ within the tumor milieu, and also generated the ROS for the re-sensitization of GBM to TMZ (Scheme 1).

Results

Nanomedicine properties

The SEM confirmed elongated morphology of TiO₂ nanosticks (Fig. 1a), whereas the DLS analyzed the average hydrodynamic size of 210 ± 23 nm size with a PDI value of



Scheme 1: Illustration of TiO₂ nanosticks-loaded temozolamide treatment and activation by ultrasound to ablate the TMZ-resistant glioblastoma multiforme. The ultrasound has a triple action therapeutic effect on GBM by (I) enhancing the nanomedicine permeability, (II) release of TMZ from TiO₂ nanosticks, and (III) generation of reactive oxygen species for sensitization of GBM to TMZ

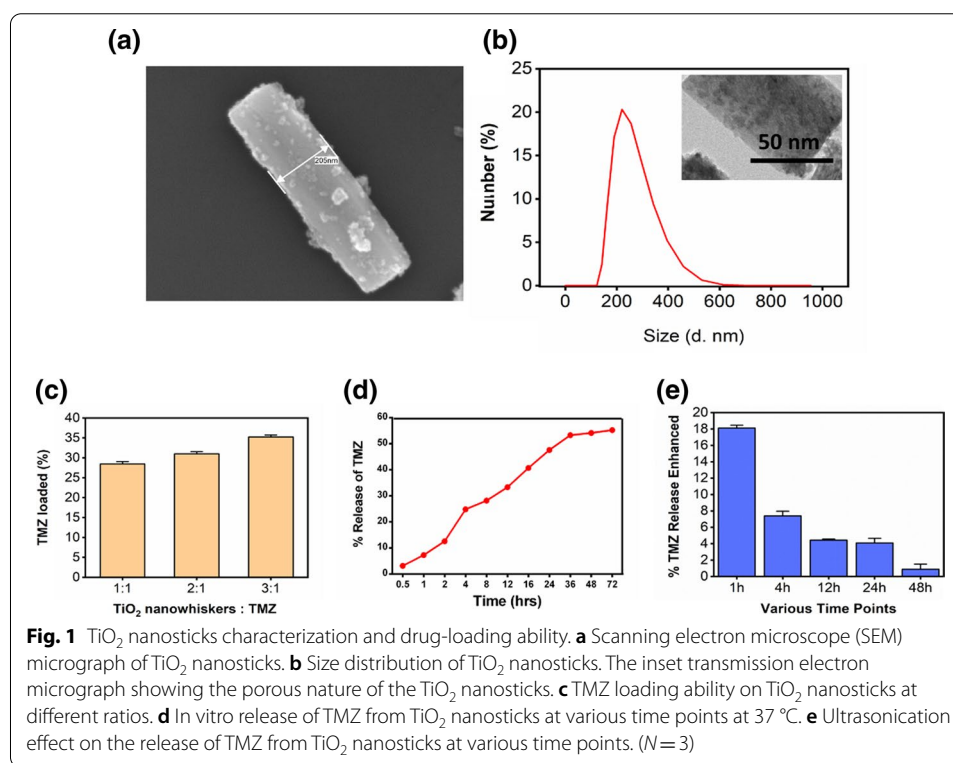


Fig. 1 TiO₂ nanosticks characterization and drug-loading ability. **a** Scanning electron microscope (SEM) micrograph of TiO₂ nanosticks. **b** Size distribution of TiO₂ nanosticks. The inset transmission electron micrograph showing the porous nature of the TiO₂ nanosticks. **c** TMZ loading ability on TiO₂ nanosticks at different ratios. **d** In vitro release of TMZ from TiO₂ nanosticks at various time points at 37 °C. **e** Ultrasonication effect on the release of TMZ from TiO₂ nanosticks at various time points. ($N=3$)

0.215 (Fig. 1b). The TEM revealed the porous nature of the TiO₂ nanosticks that played an essential role in the drug loading, as shown in Fig. 1b inset. The zeta potential of TiO₂

nanosticks was 15 ± 0.89 mV, which shows good dispersibility of the as-prepared nanomedicine (Additional file 1: Figure S1).

Drug loading/release ability

The TiO_2 nanosticks were mixed with TMZ and incubated overnight at various ratios of 1:1, 2:1, 3:1, respectively. It was observed that 3:1 (TiO_2 nanosticks: TMZ) could produce the highest drug loading, i.e., $35 \pm 3.06\%$, followed by 31 ± 2.98 and 28 ± 3.43 percent for 2:1 and 1:1, respectively (Fig. 1c). During the drug release study, it was found that after 36 h, $53 \pm 7.48\%$ of the drug was released, and no further significant increase was observed until 48 h (Fig. 1d).

After the ultrasonication, the TMZ release from TiO_2 nanosticks was evaluated. It was observed that after a 1-h time point, the sonication could trigger $18 \pm 4.89\%$ of TMZ release as compared to the non-sonicated that could only $8 \pm 4.21\%$, indicating that sonication could trigger TMZ release $2 \times$ higher than non-sonicated in a given time (Fig. 1e).

In vitro anticancer effect

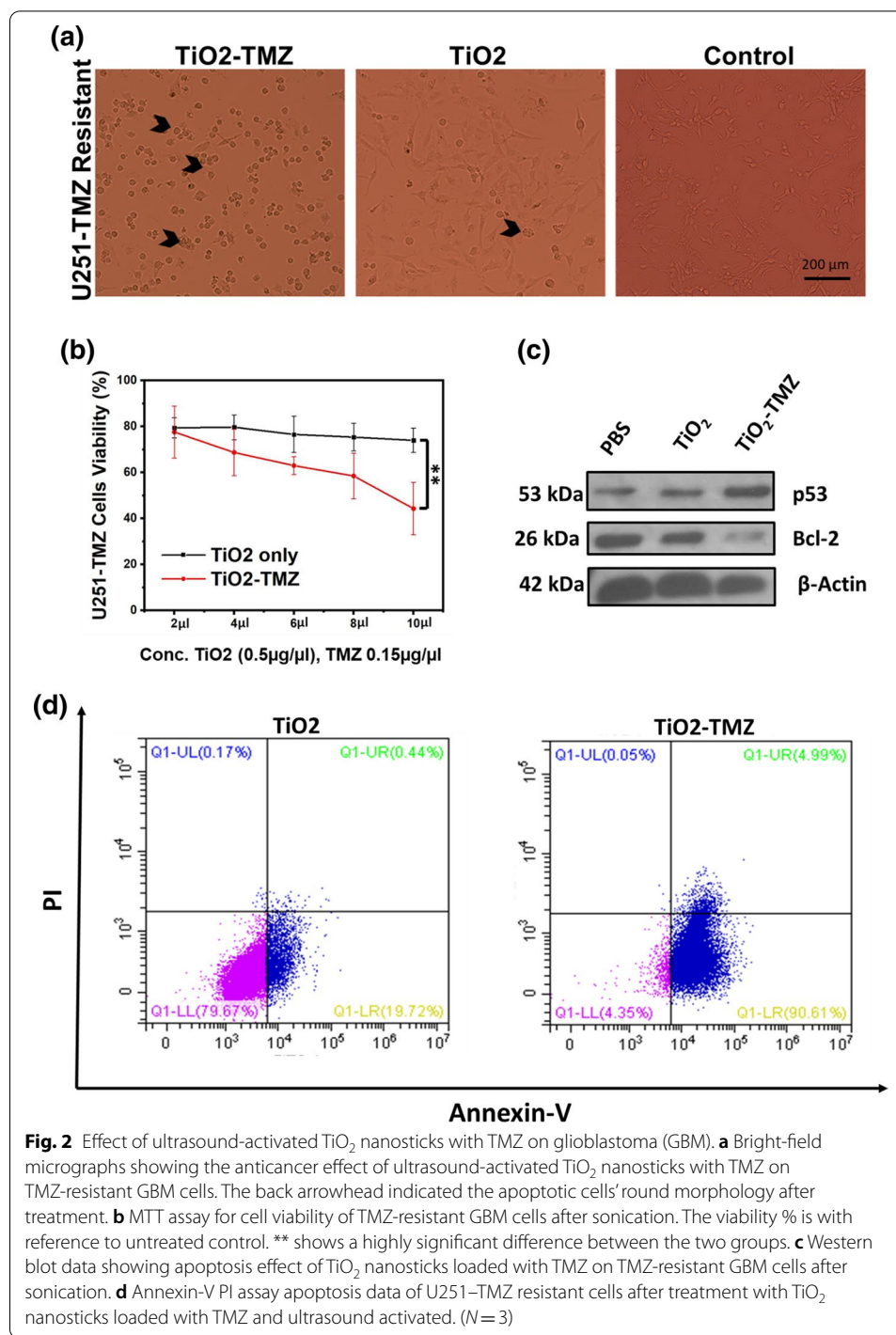
MTT assay was performed to see the anticancer effect of ultrasound-triggered TiO_2 –TMZ nanomedicine. It was observed that TiO_2 –TMZ could induce higher cell apoptosis $52.0 \pm 13.01\%$ at $10 \mu\text{L}$ of nanomedicine treatment as compared to TiO_2 alone that remained around $22 \pm 9.90\%$ at various consternations, in U251–TMZ resistant cells (Fig. 2a, b). The TiO_2 –TMZ and TiO_2 alone treatment could also induce apoptosis in TMZ-sensitive GBM cells (U87) (Additional file 1: Figure S2). Meanwhile, the non-sonicated nanomedicine could not exert any significant cytotoxic effects in U251–TMZ resistant cells, i.e., cell viability remained above 90% (Additional file 1: Figure S3).

Western blot analysis was performed for apoptosis-related vital protein expressions (P53 and Bcl-2) in TMZ-resistant GBM cells after treatment with TiO_2 –TMZ and TiO_2 alone, post-sonication. It was observed that TiO_2 –TMZ could produce a higher expression of p53, which is essential for apoptosis induction, whereas the Bcl-2 expression was significantly lowered as compared to TiO_2 -treated cells. The Bcl-2 is known for its anti-apoptosis function, and its downregulation indicates apoptosis induction (Fig. 2c).

The Annexin (v)-PI assay was also performed for apoptosis induction in the U251–TMZ-resistant cells. The flow cytometry data revealed that ultrasound-activated TiO_2 –TMZ could produce higher apoptosis than TiO_2 nanosticks alone and non-sonicated treated groups (Fig. 2d, Additional file 1: Figure S4).

Oxidative stress generated by nanomedicine

The DCFDA was used as a ROS marker of the oxidative stress in U251–TMZ resistant cells after treatment with TiO_2 –TMZ and TiO_2 in the sonicated and non-sonicated group. The confocal fluorescence microscopy revealed that TiO_2 –TMZ could generate a significantly higher number of ROS than non-sonicated and TiO_2 alone (Fig. 3a, b; Additional file 1: Figure S5). Besides, the ROS intensity was also evaluated via flow cytometry analysis, which also exhibited higher fluorescence in TiO_2 –TMZ treated groups after sonication (Fig. 3c). Meanwhile, the SOD level was also examined in the treated cells. The SOD level was significantly lowered in the TiO_2 –TMZ treated group after sonication than the non-sonicated one (Fig. 3d).



In vitro BBB-crossing ability

The BBB-crossing ability of TMZ- TiO_2 nanomedicine pre- and post-sonication was evaluated via the transwell BBB model (Fig. 4a). The EDS data revealed that TiO_2 nanosticks could readily cross the BBB after sonication and were taken up by the U251-TMZ resistant cells, as shown in Fig. 4b, c. Moreover, the TiO_2 nanosticks were loaded with Doxorubicin as a model drug having fluorescence properties. When the TiO_2 -Dox and

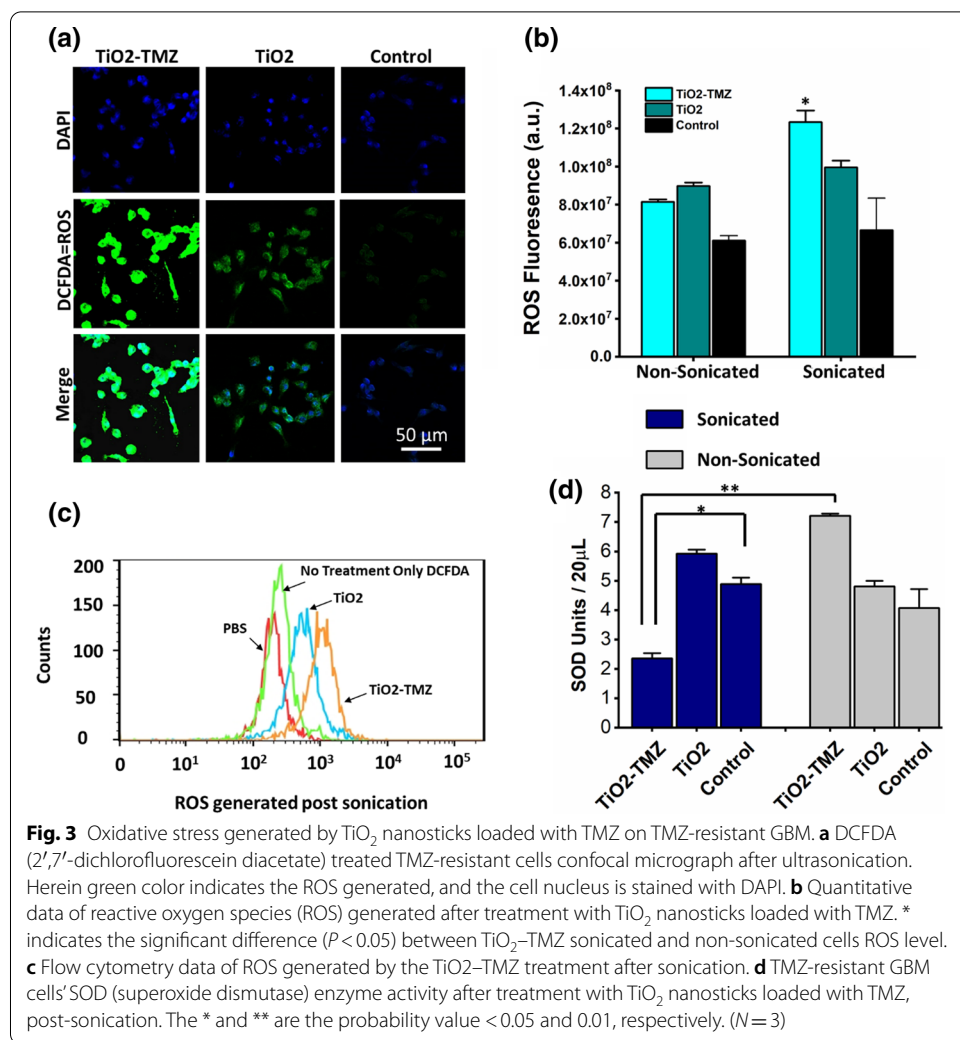


Fig. 3 Oxidative stress generated by TiO₂ nanosticks loaded with TMZ on TMZ-resistant GBM. **a** DCFDA (2',7'-dichlorofluorescein diacetate) treated TMZ-resistant cells confocal micrograph after ultrasonication. Herein green color indicates the ROS generated, and the cell nucleus is stained with DAPI. **b** Quantitative data of reactive oxygen species (ROS) generated after treatment with TiO₂ nanosticks loaded with TMZ. * indicates the significant difference ($P < 0.05$) between TiO₂-TMZ sonicated and non-sonicated cells ROS level. **c** Flow cytometry data of ROS generated by the TiO₂-TMZ treatment after sonication. **d** TMZ-resistant GBM cells' SOD (superoxide dismutase) enzyme activity after treatment with TiO₂ nanosticks loaded with TMZ, post-sonication. The * and ** are the probability value < 0.05 and 0.01, respectively. ($N = 3$)

free Dox treatment were given to the transwell BBB model, the sonication could boost the TiO₂-Dox BBB traversing, evidenced by the fluorescence intensity in the confocal fluorescence micrographs (Fig. 4d).

TiO₂ nanosticks biodistribution

At 8-h time point, the brain had the highest accumulation of the Cy5, and its signals were lowered later (Additional file 1: Figure S6). Meanwhile, the histopathology of brain and tumor suggested that cy5 strong signals were present both in the brain and tumor tissue compared to free cy5 suggesting TiO₂ nanosticks presence in brain and tumor milieu (Additional file 1: Figure S7). Likewise, the inductively coupled plasma (ICP) method was also performed for the specific biodistribution of TiO₂ nanosticks only, as shown in Additional file 1: Figure S8.

Animal model survival post-therapy

The subcutaneous xenograft mice model was initially prepared with TMZ-resistant glioblastoma cells and divided into three TiO₂-TMZ, TiO₂, and control groups. After

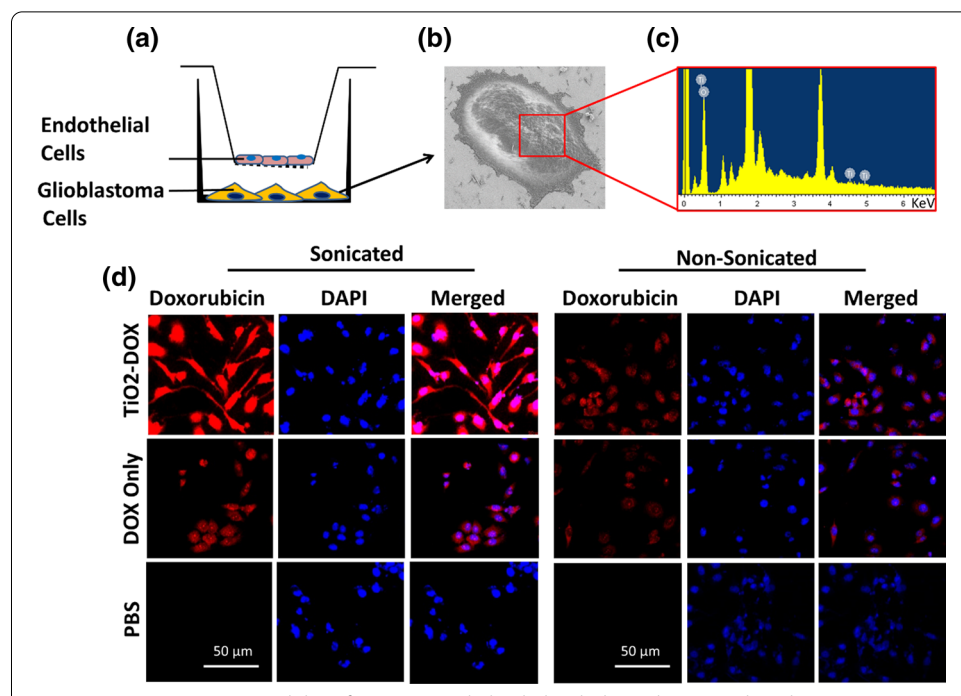


Fig. 4 In vitro BBB traversing ability of TiO_2 nanosticks loaded with doxorubicin. **a** is the schematic representation of the transwell BBB model. **b** SEM micrograph of GBM cell. **c** The energy-dispersive X-ray spectroscopy (EDS) data of transwell TiO_2 nanosticks taken by GBM-TMZ resistant cells. **d** In vitro BBB confocal fluorescence data of doxorubicin (Dox) (free and TiO_2 nanosticks loaded) with and without sonication (doxorubicin $\text{Em} = 595 \text{ nm}$)

appropriate treatments and sonication, it was observed that TiO_2 -TMZ could circumvent the tumor growth and significantly lower the tumor volume as compared to other TiO_2 alone and PBS treated groups (Fig. 5a, b). The tumor weight was significantly lowered in TMZ- TiO_2 treated groups, i.e., $0.1 \pm 0.23 \text{ g}$, as compared to TiO_2 ($0.81 \pm 0.44 \text{ g}$) and PBS group ($2.0 \pm 0.89 \text{ g}$) after sonication (Fig. 5c). Likewise, the body weight gain was higher in TMZ- TiO_2 treated group as compared to TiO_2 and control (Fig. 5d).

Similarly, the tumor volume was lower in the TiO_2 -TMZ treated models than in other treated groups (Additional file 1: Figure S9). The biodistribution data of vital body organs showed higher TMZ accumulation in the liver, i.e., the elimination route for the TMZ from the body, followed by the tumor and brain (Fig. 5e). The vital organ histopathology also revealed no pathological lesions after treatment and sonication that vouch for the biocompatibility and inertness of the as-prepared nanomedicine (Additional file 1: Figure S10).

The orthotopic TMZ-resistant GBM tumor expressing luciferase was prepared and treated with TMZ- TiO_2 at day 10 till day 21 on alternate days, as shown in the experimental layout (Fig. 5f). Meanwhile, every subsequent day of treatment, mice were imaged for bioluminescence, directly proportional to the tumor volume (Fig. 5g). The relative photon flux data showed TiO_2 -TMZ after sonication could circumvent the tumor volume more efficiently than other treated groups (Fig. 5h). The animal treated with TMZ- TiO_2 had the highest survival rate (56 days) post-therapy compared to other groups (Fig. 5i).

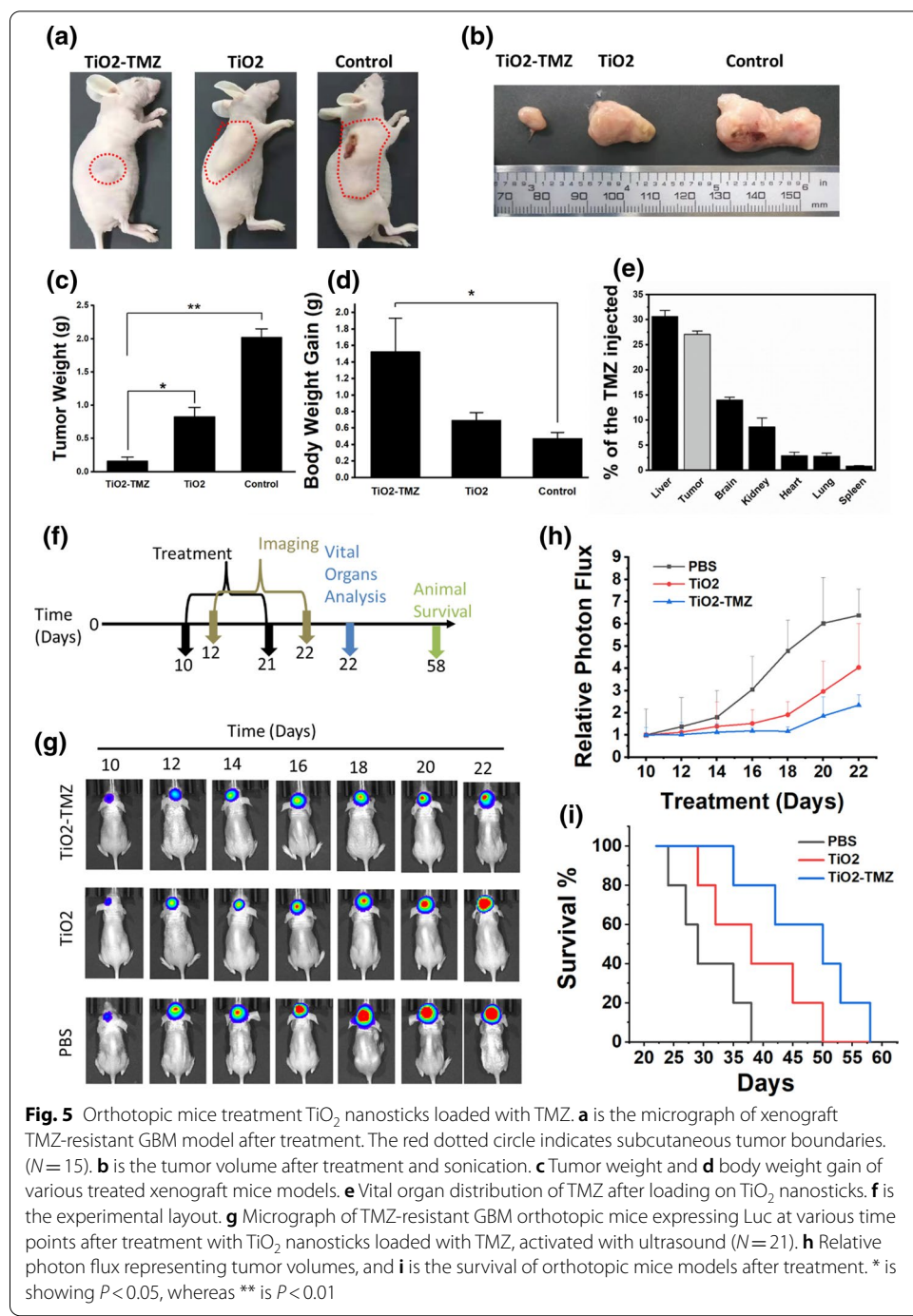


Fig. 5 Orthotopic mice treatment TiO_2 nanosticks loaded with TMZ. **a** is the micrograph of xenograft TMZ-resistant GBM model after treatment. The red dotted circle indicates subcutaneous tumor boundaries. ($N=15$). **b** is the tumor volume after treatment and sonication. **c** Tumor weight and **d** body weight gain of various treated xenograft mice models. **e** Vital organ distribution of TMZ after loading on TiO_2 nanosticks. **f** is the experimental layout. **g** Micrograph of TMZ-resistant GBM orthotopic mice expressing Luc at various time points after treatment with TiO_2 nanosticks loaded with TMZ, activated with ultrasound ($N=21$). **h** Relative photon flux representing tumor volumes, and **i** is the survival of orthotopic mice models after treatment. * is showing $P < 0.05$, whereas ** is $P < 0.01$

Discussion

GBM is one among the fatal brain diseases. Its complete resection is still a challenge with only TMZ as an available chemotherapeutic agent. In addition, the frequent resistance development to TMZ has further complicated GBM cure (Casals et al. 2017). In this contribution, we have employed ultrasound-activated TiO_2 nanosticks loaded with TMZ to resect the TMZ-resistant GBM *in vitro* and *in vivo*. The ultrasound trigger has a triple action effect aiding to GBM resection by: (i) opening BBB, (ii) releasing TMZ

payload from TiO_2 nanosticks, and (iii) ROS generation from TiO_2 nanosticks that helps in re-sensitization of GBM to TMZ (You et al. 2016). Previously, the nanoscale TiO_2 sonication at 1.0 MHz frequency has been reported with efficient intratumor ROS generation that inhibited cell viability and tumor growth (Harada et al. 2011). Herein, we have employed a 1.5-MHz frequency ultrasound that could efficiently penetrate the skull bones of orthotopic GBM models. The typical diagnostic and materials application ultrasound range from 1 to 10 MHz frequency (Silva et al. 2011). Hence, the employed ultrasound modality is in line with therapeutic ultrasound in vogue.

The TiO_2 nanosticks can upload maximum TMZ at a ratio of 3:1. The TMZ has been adsorbed on the porous surface of TiO_2 nanosticks after overnight incubation, the same as previously reported (Rehman et al. 2016a, b). Interestingly, it was observed that ultrasonication could trigger the drug release much faster than non-sonicated TiO_2 . Likewise, Shi et al. loaded docetaxel on the mesoporous TiO_2 nanoparticles to treat cancer via sonodynamic therapy (Shi et al. 2015). It was observed that docetaxel-loaded TiO_2 could significantly deliver and release the drug in the tumor site after sonication and exhibited excellent anticancer efficacy. Moreover, the TMZ has a natural ability to cross the BBB, as earlier reported (Brun et al. 2012). However, when the ultrasound is employed in the BBB, the nanomedicine traversing becomes faster with maximum drug bioavailability in brain tissue.

This study has used two-step ultrasonication in orthotopic animal models; the first one is to open the BBB for nanomedicine traversing that ensures maximum drug accumulation within the brain tissue. The second sonication ensures the quick releases of TMZ from TiO_2 nanosticks and also starts ROS generation. The ultrasound-activated TiO_2 can generate OH , ${}^1\text{O}_2$, H_2O_2 , etc., which interferes with cell signal pathways and initiates apoptosis or necrosis within the target tissue (Ninomiya et al. 2012). Likewise, Harada et al. (2013) sonoactivated nanoscale TiO_2 that, as a consequence, released ${}^1\text{O}_2$, which is widely considered most cytotoxic ROS after sonodynamic therapy. Meanwhile, Dai et al. (2017) employed 1,3 diphenylisobenzofuran (DPBF) as a typical molecular probe to quench ${}^1\text{O}_2$. It was revealed that TiO_2 -based nanosystems, after sonication, could release a considerable amount of cytotoxic ${}^1\text{O}_2$.

In this study, when TMZ-resistant GBM cells were treated with as-prepared nanomedicine, the sonication effect could produce less than 50% cell viability.

Moreover, the critical apoptosis markers (P53 and Bcl-2) were significantly influenced by the sonicated nanomedicine. Earlier, Zhang et al. (2010) reported that TMZ induces O^6 -methylguanine production involved in AMP-activated protein kinase (AMPK) activation via an elevated level of ROS generated. The AMPK is involved in the GBM apoptosis induction via p53 upregulation. Meanwhile, by inhibiting mTOR complex 1, the Bcl-2 protein expression is downregulated, further inducing TMZ-mediated pro-apoptotic effect. Likewise, Kim et al. (2015) also reported the tumor-targeting p53 nano-drug delivering system enhanced sensitization of chemoresistant GBM to TMZ therapy. In analogy to TMZ, the TiO_2 also generates ROS, resulting in AMPK activation and apoptosis induction in TMZ-resistant GBM. The sonoluminescence is considered a critical phenomenon to generate ROS from nanoscale TiO_2 (Hu et al. 2015), that on the one hand, induces apoptosis in the tumor (You et al. 2016) and, on the other hand, destroy

the tumor vasculature endothelial layer or blood stasis via platelet aggregation (Borsig et al. 2001; Volanti et al. 2004).

Three treatment groups of TMZ–TiO₂, TiO₂, and control were either sonicated or non-sonicated. The data shows a significantly elevated level of ROS generated after sonication in TMZ–TiO₂ treated groups. Likewise, when the TMZ–TiO₂ group was sonicated, the ROS generated were above the SOD threshold within the treated cells, which resulted in cease of cell activities and resulted in cell apoptosis; consequently, lesser SOD was detected as compared to TiO₂ alone. In comparing TiO₂ sonicated and non-sonicated, it is evident that TiO₂ sonicated has a higher number of SOD generated, which indicated the higher level of ROS after sonication. Likewise, let us compare the SOD level within TMZ–TiO₂ sonicate and non-sonicate group. The ROS level is significantly higher than other treatment groups, and due to apoptosis induced within cells, no further SOD is produced.

In a recent study, Feng et al. (2016), employed the NAMPT inhibitors (FK866, CHS828) and TMZ to sensitize the GBM cells to TMZ. In addition to other factors, these NAMPT inhibitors could elevate the ROS level and reduce the SOD and total anti-oxidants activity in GBM cells to sensitize the GBM cells to TMZ. Likewise, Seyfrid et al. (2016) employed Smac mimetic (BV6) and TMZ to sensitize the GBM to chemotherapy. The combination therapy of BV6–TMZ could orchestrate the ROS generation in the mitochondria and cytosolic contents of GBM. These ROS could then activate the pro-apoptotic factors viz Bax protein upregulation to resect GBM. It has been investigated that TMZ could induce cytoprotective autophagy in GBM cells, thus leading to compromised TMZ sensitivity. However, when mitochondria transport chain inhibitors are combined with TMZ as adjuvant therapy, the autophagic cell death is mediated by ROS (Chen et al. 2007), and GBM sensitivity to TMZ is significantly augmented (Yan et al. 2016). Our findings are also in agreement with the aforementioned results suggesting that elevated ROS level and decreased antioxidant level (i.e., SOD) ensures the re-sensitization of GBM to TMZ. Thus, apoptosis is initiated in the GBM.

Conclusion

In summary, we report that TiO₂ nanosticks could significantly deliver the TMZ payload to the brain milieu across the BBB and resect the TMZ-resistant GBM. The ultrasonication triple-action effect could open the BBB, release the TMZ from TiO₂ nanosticks, and mimic the ROS generation within GBM. The generated ROS enhances the tumor sensitivity to TMZ that resulting in apoptosis induction and tumor growth arrest in *in vitro* and xenograft and orthotopic TMZ-resistant GBM models. The reported modality is novel and reported for the first time (as per our knowledge).

Methods

All the chemicals used in this study were experimental grade and purchased from Sigma Aldrich (St. Louis, Missouri, USA), otherwise mentioned. The Milli-Q deionized water with $-18\text{m}\Omega/\text{cm}^2$ was used to prepare chemical reagents. HyClone Inc. USA provided the cell culture media and reagents, whereas the cell culture flasks were purchased from Nest biotechnologies Wuxi, China. The TiO₂ nanosticks were kindly provided by Dr.

Xiao Hua Lu, College of Engineering, Nanjing University of Technology, Nanjing, China. The details of the TiO_2 nanosticks preparation can be followed in Li et al. (2008).

All the animals were provided with pellet feed and water ad libitum in an environmentally controlled house. All the experiments were performed under the guidelines of the Henan University animal welfare committee.

Materials characterization

The TiO_2 nanosticks were morphologically characterized by Scanning and transmission electron microscopy (Jeol, the USA, and JEM-2010HT Japan, respectively). The size and zeta potential of materials was performed by using Zetasizer Nano (Malvern Panalytical Ltd.). SEM performed the energy-dispersive X-ray spectroscopy (EDS) to see cell uptake of TiO_2 nanosticks after crossing BBB in vitro.

Nanomedicine preparation

The TiO_2 nanosticks 0.5 mg/mL and TMZ 0.45 mg/mL were dissolved in the deionized distilled water and then mixed and kept at room temperature on a magnetic stirrer for overnight rotation. Then the solution was centrifuged at $8000 \times g$ for 10 min to remove unbound TMZ from TiO_2 nanosticks. The TiO_2 nanosticks were then washed with deionized distilled water and stored in PBS with a final concentration of TiO_2 (0.5 mg/mL): TMZ (0.15) mg/mL.

Drug loading and releases

The TiO_2 nanosticks 1 mg/mL and TMZ 1 mg/mL were dissolved in deionized water and then mixed at the various concentration ratios of 1:1, 2:1, and 3:1. The TMZ concentration was kept constant, whereas the TiO_2 nanosticks ratio was variable. Above 3:1, no significant difference was observed. The TiO_2 -TMZ mixture was kept on rotation overnight at room temperature and then centrifuged at $8000 \times g$ to remove untrapped TMZ. The TMZ absorption value was determined at 327 nm to determine the TMZ uploading value on TiO_2 nanosticks.

The release kinetics of TiO_2 -TMZ nanomedicine was performed at 37 °C in PBS. At various time points of 0.5, 1, 2, 4, 8, 12, 16, 24, 36, 48, and 72 h the centrifugation was performed ($8000 \times g$), and TMZ concentration was measured by taking absorbance value at 327 nm. For sonication effect on TMZ releases, at a time point of 1, 4, 12, 24, and 48 h, after incubation, the sonication was performed, i.e., 1.0 Watt/cm², 1.5 MHz frequency with 50% intensity by intellect mobile ultrasound (Chattanooga®, GLOBAL DJO HEADQUARTERS 2900 Lake Vista Drive Dallas, TX 75067) and then reading for TMZ concentration was performed.

Cell culture experiments

The U87 cell line of glioblastoma and b.End3 cell line of endothelial cells was provided by the Chinese Academy of Sciences, Shanghai, China. The U251 cells were TMZ resistant and transfected with luciferase were obtained from iCell Bioscience Inc., Shanghai, China. The cells were cultured in the 25 cm² tissue culture flasks in DMEM high glucose medium supplemented with 10% FBS and 1% penicillin–streptomycin solution under standard incubation conditions of 95% relative humidity at 37 °C temperature, in the

presence of 5% CO₂. When the confluence reached 90%, the cells were trypsinized with 0.25% trypsin containing EDTA and were further utilized for downstream experiments.

Western blot

The western blot technique was employed to evaluate the apoptotic protein biomarkers (Bcl-2 and p53) and housekeeping genes β-actin by the procedure mentioned earlier (Haney et al. 2015). The Bcl-2 and p53 primary rabbit anti-human antibodies were provided by Biolegend and diluted to a concentration of 1:5000. In contrast, secondary antibodies (IRDye 800CW goat anti-rabbit secondary antibodies) were provided by LI-COR Biosciences U.S. The protein bands were visualized by Odyssey® Clx western blot scanner (LI-COR Biosciences—U.S.) and processed by image studio software.

Flow cytometry for apoptosis

U251-TMZ resistant cells were cultured in 10 cm Petri dishes for 24 h under standard conditions. The cells were divided into five groups, i.e., PBS, TiO₂ only, TiO₂-TMZ, TiO₂ sonicated, TiO₂-TMZ sonicated, and treatment for another 12 h. Meanwhile, after one hour of inoculation, the two groups, i.e., TiO₂ sonicated and TiO₂-TMZ sonicated, were sonicated for one minute. Afterward, the cells were trypsinized and treated with Annexin(v)-PI reagent (Beyotime Biotech Inc.) for cell apoptosis evaluation according to manufacturer instructions. The cells were then immediately analyzed through the BD FACS Aria flow cytometer for apoptosis detection.

MTT assay for cytotoxicity

U251-TMZ resistant cells were cultured in 96 well plates at an equal concentration of 1×10^3 cell per mL for 24 h. The cells were treated with TiO₂ only, TiO₂-TMZ, sonicated, and non-sonicated groups, whereas the control group was treated with PBS for 24 h with concentration from 1 to 10 µg of nanomedicine per well. The ultrasound group was sonicated for one minute after one hour of nanomedicine inoculation by sonication procedure mentioned earlier. Afterward, 20 µL of 5 mg/mL of MTT solution was added to each well and incubated for 4 h. Then the medium was discarded, and 200 µL of DMSO was added to each well and incubated for 10 min at room temperature. The plates were then subject to an optical density (OD) reading at 492 nm wavelength by ELISA microplate reader (SpectraMax® i3x, Molecular Devices, LLC).

The following formula evaluated the cell viability:

$$\text{Cell viability (\%)} = \frac{\text{OD value of treatment}}{\text{OD value of Control}} \times 100.$$

Confocal microscopy

The U251-TMZ resistant cells were cultured for 24 h on the confocal microscopy Petri dishes provided with the lens at the bottom. The cells were then divided into two main groups, i.e., sonicated and non-sonicated. These groups were further divided into TiO₂, TiO₂-TMZ, and PBS. Each group was inoculated with corresponding nanomedicine @ 10 mg/mL and further incubated for 12 h; meanwhile, the sonicated group was ultrasound treated 1-h post-nanomedicine inoculation. The cells were then treated with a 2',7'-dichlorodihydrofluorescein diacetate (DCFDA) reagent (Invitrogen™) 1% solution

for one hour. Afterward, the cells were washed with PBS 3 times and added DAPI solution 1:1000 for five minutes to stain the cell nucleus. Again, after washing, the cells were fixed with paraformaldehyde 4% for 10 min. Then washed again with PBS and imaged under a confocal microscope (Zeiss LSM 880) at the FITC channel, whereas the cell nucleus was imaged at the DAPI channel.

For quantitative ROS analysis, the DCFDA treated medium from cells was collected after one hour of incubation, and fluorescence was measured at 488 nm wavelength using SpectraMax® i3x, Molecular Devices, LLC.

In vitro BBB model preparation

The endothelial cells were cultured on the transwell membrane (Millicell®, 100 nm pore size) until the complete cell confluence was achieved, and the cells' conductivity resistance become above $300\ \Omega$. Then U251-TMZ resistant cells were cultured on the lower chamber of the 12 well plate containing round glass coverslips, and treatment of (Doxorubicin) DOX, TiO_2 -DOX, and PBS was given to sonicated and non-sonicated group @ 10 mg/mL of corresponding nanomedicine. After one hour, the sonicated group was ultrasound treated as mentioned above and incubated under standard incubation conditions with 100 rotations per minute (to generate sufficient shear force) for 12 h. Later the cell culture medium was removed and washed with PBS, then added 1:1000 DAPI solution for 5 min to stain the cell nucleus. Afterward, the cells were washed with PBS and fixed with paraformaldehyde 4% for 10 min. The glass coverslips were removed from the 12 well plates and mounted on the glass slide to observe under a confocal microscope.

SOD activity

The U251-TMZ resistant cells were cultured in six-well plates. When the cell confluence reached 90%, they were divided into two groups, i.e., sonicated and non-sonicated. Both groups were separately treated with TiO_2 and TiO_2 -TMZ @ 10 mg/mL, whereas the PBS group was kept as control. The sonicated group, after one hour, was treated with ultrasound, as mentioned above. After overnight incubation, the Superoxide Dismutase level was determined in each group from the cell lysate by the commercially available kit (SOD Assay Kit-WST, Dojindo Molecular Technologies, Inc.) following the manufacture instructions. A microplate reader was used to read the optical density value at 450 nm wavelength.

Xenograft and orthotopic animal models preparation

Luciferin expressing U251-TMZ resistant cells were cultured in the 75-cm² culture flasks. After attaining 90% confluence, the cells were trypsinized (0.25% trypsin) and collected in pellet form. These cells were then injected into BALB/C athymic nude mice @ 3×10^6 cells subcutaneously to form tumors. After 2 weeks, a palpable size of the tumor was noticed. These mice were then used for further experiments, whereas few were euthanized to obtain the tumor for orthotopic model preparation.

The tumor was chopped to a small size in normal saline and injected into a mouse brain exposed by a skull puncture under general anesthesia of isoflurane. The skull bone was then sealed with a bone sealant (CP Medical), and the wound was sealed via tissue adhesive glue (Vetbond™, 3 M, Japan). On day 3, mice were imaged for bioluminescence

by IVIS-Lumina Series III, PerkinElmer Inc, after injection of D-luciferin solution (5 mg/mL). The successful models showing bioluminescence were further selected for experimental trials.

Animal treatment

The subcutaneous xenograft GBM TMZ-resistant mice were divided into three groups (i.e., TiO₂, TMZ–TiO₂, and a control group treated with PBS. $N=5 \times 3$). On day 21 of the first implant, the mice were treated with as-prepared TiO₂ and TMZ solution @ dose rate of 200 μL, either separately or in combination, every alternate day for 15 days. Thirty minutes post-injection, ultrasound therapy was given at the tumor site. Then mice were euthanized, and vital organs (liver, kidney, spleen, lungs, brain) and tumor were removed and further analyzed.

The three groups of orthotopic mice were injected with the nanomedicine (200 μL) on days 10–22, every alternate day. Post-injection every 10 min, followed by 30 min, the ultrasound therapy at the head region was performed ($N=7 \times 3$). Meanwhile, the mice were imaged for bioluminescence every subsequent day of treatment during the experimental trial, and the relative photon flux value was recorded. Animal survival was also recorded daily.

TMZ biodistribution

A group of orthotopic tumor mice ($N=3$) was given the treatment of TMZ–TiO₂, i.e., 200 μL dissolved in PBS were injected into mice through the tail vein. After 12 h, the vital organs were removed after euthanasia, weighed, and homogenized (by using JXF-STPRP-48) in the presence of DMSO and 1% Triton X solution, 200 μL each. After overnight dark incubation, the homogenized organs were centrifuged at 15,000×g for 30 min, and the supernatant absorbance value was read at 327 nm in a microplate reader.

ICP for TiO₂ biodistribution

A group of orthotopic mice ($N=6$) was treated with TiO₂ nanosticks 200 μL through the tail vein. At several time points of 0 (control), 2, 12, 24 h, the animals were euthanized, and vital organs and tumor were removed, homogenized, and analyzed through ICP for total Ti ions concentration present that was directly proportional to the biodistribution of cargo.

Cy5 dye conjugation with TiO₂ nanosticks

The TiO₂ nanosticks were conjugated with Cy5 by incubating it with TiO₂ overnight at room temperature and 800 rpm. Later the TiO₂ nanosticks were washed three times with deionized water at 10,000 rpm for 10 min. The TiO₂–Cy5 and free Cy5 were then resuspended in the PBS, injected into the xenograft tumor mice, and imaged at various time points (0, 1, 2, 4, 8, 12, 24 h). After euthanasia, the brain was removed, and tissue slides were prepared and imaged under the confocal microscope for Cy5 presence (Cy-5 excitation was 630 nm and emission at 670 nm wavelengths).

Histopathology

The mice's vital organs were collected and preserved in the 10% formalin solution. Then paraffin embedding technique was used to prepare 3 μm slides, stained them with hematoxylin and eosin, and observed under an Olympus fluorescence microscope for histopathological lesion observations.

Statistical analysis

All the data were initially recorded in the MS-Excel and then subjected to analysis of variance (ANOVA) using statistical software named SPSS version 18 (SPSS Inc. Chicago Illinois USA). All results presented were in mean \pm standard deviation (SD). The probability value < 0.05 was considered statistically significant.

Supplementary Information

The online version contains supplementary material available at <https://doi.org/10.1186/s12645-021-00088-6>.

Additional file 1: **Figure S1.** Zeta potential of TiO_2 nanosticks. **Figure S2.** U87 cell micrograph showing the TMZ-sensitive cells (U87) morphology after ultrasonication. The arrowhead is indicating apoptotic cells post-therapy. **Figure S3.** cell viability of TMZ-resistant (U251) cells without ultrasonication. **Figure S4.** Annexin-V PI flow cytometry data of non-sonicated treatment groups in TMZ-resistant GBM cells. **Figure S5.** Oxidative stress (ROS) generated in TMZ resistant cells (U251) confocal micrograph after treatment with TiO_2 nanosticks loaded with TMZ without sonication. The ROS is represented by green fluorescence generated by DCFDA, whereas the cell's nucleus is stained with DAPI. The scale bar is 50 μm . **Figure S6.** showing brain accumulation of TiO_2 -Cy5 nanosticks at various time points. **Figure S7.** showing xenograft brain tissue confocal micrograph for cy5 accumulation, i.e., directly proportional to the TiO_2 nanosticks accumulation in the tissue. Red fluorescence is Cy5 and Blue is DAPI. The scale bar is 50 μm . **Figure S8.** ICP method used to explore the TiO_2 nanosticks biodistribution in vital organs and tumor in orthotopic xenograft murine models. **Figure S9.** In vivo xenograft models tumor volume after treatment with ultrasound-activated TiO_2 nanosticks loaded with TMZ. * is representing the significance level $p < 0.05$ between TiO_2 -TMZ and control group. **Figure S10.** Vital organs histopathology after treatment with sonicated TiO_2 and TiO_2 -TMZ. The organs were stained with Hematoxylin and Eosin stain. The scale bar is 200 μm .

Acknowledgements

We acknowledge the China postdoctoral foundation.

Authors' contributions

FUR and MAR designed and conducted the experiments. SU performed orthotopic xenograft animal model preparations. SS and AQ performed the cell experiments. PM and SH performed animal experiments. FUR also analyzed the data and prepared the manuscript. All authors read and approved the final manuscript.

Funding

Not applicable.

Availability of data and materials

The data sets generated and/or analysis during this study are available from the corresponding author upon request.

Declarations

Ethics approval and consent to participate

Not applicable.

Consent for publication

Not applicable.

Competing interests

The authors declare that they have no competing interests.

Author details

¹International Joint Centre for Biomedical Innovations, School of Life Sciences, Henan University, Jin Ming Avenue, Kaifeng 475004, Henan, China. ²Barbara Ann Karmanos Cancer Institute, Wayne State University Detroit, Detroit, MI, USA.

³Department of Neurosurgery, Khyber Teaching Hospital, Peshawar, Pakistan. ⁴State Key Laboratory of Bioelectronics, Chien-Shiung Wu Lab, School of Biological Science and Medical Engineering, Southeast University, Nanjing 210096, China.

Received: 7 August 2020 Accepted: 30 June 2021

Published online: 10 July 2021

References

- Abbott NJ, Rönnbäck L, Hansson E. Astrocyte–endothelial interactions at the blood–brain barrier. *Nat Rev Neurosci*. 2006;7:41.
- Bahadur S, Sahu AK, Baghel P, Saha S. Current promising treatment strategy for glioblastoma multiform: a review. *Oncol Rev*. 2019;13:417.
- Bing C, Hong Y, Hernandez C, Rich M, Cheng B, Munaweera I, et al. Characterization of different bubble formulations for blood–brain barrier opening using a focused ultrasound system with acoustic feedback control. *Sci Rep*. 2018;8:1–12.
- Borsig L, Wong R, Feramisco J, Nadeau DR, Varki NM, Varki A. Heparin and cancer revisited: mechanistic connections involving platelets, P-selectin, carcinoma mucins, and tumor metastasis. *Proc Natl Acad Sci USA*. 2001;98:3352–7.
- Brun E, Carrière M, Mabondzo A. In vitro evidence of dysregulation of blood–brain barrier function after acute and repeated/long-term exposure to TiO₂ nanoparticles. *Biomaterials*. 2012;33:886–96.
- Casals E, Gusta MF, Cobaleda-Siles M, Garcia-Sanz A, Puntes VF. Cancer resistance to treatment and antiresistance tools offered by multimodal multifunctional nanoparticles. *Cancer Nanotechnol*. 2017;8:7.
- Chamberlain MC. Temozolomide: therapeutic limitations in the treatment of adult high-grade gliomas. *Expert Rev Neurother*. 2010;10:1537–44.
- Chen Y, McMillan-Ward E, Kong J, Israels SJ, Gibson SB. Mitochondrial electron-transport-chain inhibitors of complexes I and II induce autophagic cell death mediated by reactive oxygen species. *J Cell Sci*. 2007;120:4155–66.
- Dai C, Zhang S, Liu Z, Wu R, Chen Y. Two-dimensional graphene augments nanosensitized sonocatalytic tumor eradication. *ACS Nano*. 2017;11(9):9467–80.
- Deepagan V, You DG, Um W, Ko H, Kwon S, Choi KY, et al. Long-circulating Au-TiO₂ nanocomposite as a sonosensitizer for ROS-mediated eradication of cancer. *Nano Lett*. 2016;16:6257–64.
- Feng J, Yan P-F, Zhao H-Y, Zhang F-C, Zhao W-H, Feng M. Inhibitor of nicotinamide phosphoribosyltransferase sensitizes glioblastoma cells to temozolomide via activating ROS/JNK signaling pathway. *BioMed Res Int*. 2016. <https://doi.org/10.1155/2016/1450843>.
- Haar CP, Hebbal P, Wallace GC, Das A, Vandegrift WA, Smith JA, et al. Drug resistance in glioblastoma: a mini review. *Neurochem Res*. 2012;37:1192–200.
- Haney MJ, Klyachko NL, Zhao Y, Gupta R, Plotnikova EG, He Z, et al. Exosomes as drug delivery vehicles for Parkinson's disease therapy. *J Controlled Release*. 2015;207:18–30.
- Harada Y, Ogawa K, Irie Y, Endo H, Feril LB Jr, Uemura T, et al. Ultrasound activation of TiO₂ in melanoma tumors. *J Controlled Release*. 2011;149:190–5.
- Harada A, Ono M, Yuba E, Kono K. Titanium dioxide nanoparticle-entrapped polyion complex micelles generate singlet oxygen in the cells by ultrasound irradiation for sonodynamic therapy. *Biomater Sci*. 2013;1:65–73.
- Hu Z, Fan H, Lv G, Zhou Q, Yang B, Zheng J, et al. 5-Aminolevulinic acid-mediated sonodynamic therapy induces anti-tumor effects in malignant melanoma via p53-miR-34a-Sirt1 axis. *J Dermatol Sci*. 2015;79:155–62.
- Iqbal Y, Mustafa MK, Wang J, Wang C, Majeed U, Muhammad P, Rehman FU, Ahmad I. Synthesis and growth mechanism of ZnO nanospheres by hydrothermal process and their anticancer effect against glioblastoma multiforme. *Biomed Lett*. 2020;6:17–22.
- Kim S-S, Rait A, Kim E, Pirolli KF, Chang EH. A tumor-targeting p53 nanodelivery system limits chemoresistance to temozolomide prolonging survival in a mouse model of glioblastoma multiforme. *Nanomedicine*. 2015;11:301–11.
- Li W, Liu C, Zhou Y, Bai Y, Feng X, Yang Z, Lu L, Lu X, Chan KY. Enhanced photocatalytic activity in anatase/TiO₂ (B) core–shell nanofiber. *J Phys Chem C*. 2008;112:20539–45.
- Lipsman N, Meng Y, Bethune AJ, Huang Y, Lam B, Masellis M, et al. Blood–brain barrier opening in Alzheimer's disease using MR-guided focused ultrasound. *Nat Commun*. 2018;9:1–8.
- Liu H-L, Huang C-Y, Chen J-Y, Wang H-YJ, Chen P-Y, Wei K-C. Pharmacodynamic and therapeutic investigation of focused ultrasound-induced blood-brain barrier opening for enhanced temozolomide delivery in glioma treatment. *PLoS ONE*. 2014;9: e114311.
- Mi Y, Shao Z, Vang J, Kaidar-Person O, Wang AZ. Application of nanotechnology to cancer radiotherapy. *Cancer Nanotechnol*. 2016;7:1–16.
- Mitragotri S. Devices for overcoming biological barriers: the use of physical forces to disrupt the barriers. *Adv Drug Deliv Rev*. 2013;65:100–3.
- Ninomiya K, Ogino C, Oshima S, Sonoke S, Kuroda S-i, Shimizu N. Targeted sonodynamic therapy using protein-modified TiO₂ nanoparticles. *Ultrason Sonochem*. 2012;19:607–14.
- Ninomiya K, Noda K, Ogino C, Kuroda S-i, Shimizu N. Enhanced OH radical generation by dual-frequency ultrasound with TiO₂ nanoparticles: its application to targeted sonodynamic therapy. *Ultrason Sonochem*. 2014;21:289–94.
- Pardridge WM. Blood–brain barrier delivery. *Drug Discov Today*. 2007;12:54–61.
- Patel AP, Fisher JL, Nichols E, Abd-Allah F, Abdela J, Abdelalim A, et al. Global, regional, and national burden of brain and other CNS cancer, 1990–2016: a systematic analysis for the global burden of disease study 2016. *Lancet Neurol*. 2019;18:376–93.
- Rehman FU. Impact of bioinspired nanotechnology on brain diseases amelioration. *Biomed Lett*. 2020;6:17–22.
- Rehman F, Zhao C, Jiang H, Wang X. Biomedical applications of nano-titania in theranostics and photodynamic therapy. *Biomat Sci*. 2016;4:40–54.
- Rehman FU, Zhao C, Wu C, Li X, Jiang H, Selke M, et al. Synergy and translation of allogenic bone marrow stem cells after photodynamic treatment of rheumatoid arthritis with tetra sulfonatophenyl porphyrin and TiO₂ nanowhiskers. *Nano Res*. 2016;9:3305–21.

- Seyfrid M, Marschall V, Fulda S. Reactive oxygen species contribute toward Smac mimetic/temozolomide-induced cell death in glioblastoma cells. *Anticancer Drugs*. 2016;27:953–9.
- Shi J, Chen Z, Wang B, Wang L, Lu T, Zhang Z. Reactive oxygen species-manipulated drug release from a smart envelope-type mesoporous titanium nanovehicle for tumor sonodynamic-chemotherapy. *ACS Appl Mater Interfaces*. 2015;7:2854–65.
- Silva R, Ferreira H, Cavaco-Paulo A. Sonoproduction of liposomes and protein particles as templates for delivery purposes. *Biomacromol*. 2011;12:353–68.
- Srikanth M, Kessler JA. Nanotechnology—novel therapeutics for CNS disorders. *Nat Rev Neurol*. 2012;8:307.
- Volanti C, Gloire G, Vanderplaschen A, Jacobs N, Habraken Y, Piette J. Downregulation of ICAM-1 and VCAM-1 expression in endothelial cells treated by photodynamic therapy. *Oncogene*. 2004;23:8649–58.
- Wu S-Y, Aurup C, Sanchez CS, Grondin J, Zheng W, Kamimura H, et al. Efficient blood-brain barrier opening in primates with neuronavigation-guided ultrasound and real-time acoustic mapping. *Sci Rep*. 2018;8:1–11.
- Xu H, Chen J, Xu H, Qin Z. Geographic variations in the incidence of glioblastoma and prognostic factors predictive of overall survival in US adults from 2004–2013. *Front Aging Neurosci*. 2017;9:352.
- Yan Y, Xu Z, Dai S, Qian L, Sun L, Gong Z. Targeting autophagy to sensitive glioma to temozolamide treatment. *J Exp Clin Cancer Res*. 2016;35:23.
- You DG, Deepagan V, Um W, Jeon S, Son S, Chang H, et al. ROS-generating TiO₂ nanoparticles for non-invasive sonodynamic therapy of cancer. *Sci Rep*. 2016;6:1–12.
- Youssef Z, Vaudreuil R, Colombeau L, Baros F, Roques-Carmes T, Frochot C, et al. The application of titanium dioxide, zinc oxide, fullerene, and graphene nanoparticles in photodynamic therapy. *Cancer Nanotechnol*. 2017;8:6.
- Zhang W-b, Wang Z, Shu F, Jin Y-h, Liu H-y, Wang Q-j, et al. Activation of AMP-activated protein kinase by temozolamide contributes to apoptosis in glioblastoma cells via p53 activation and mTORC1 inhibition. *J Biol Chem*. 2010;285:40461–71.
- Zhao C, Ur Rehman F, Yang Y, Li X, Zhang D, Jiang H, et al. Bio-imaging and photodynamic therapy with tetra sulphonatophenyl porphyrin (TSPP)-TiO₂ nanowhiskers: new approaches in rheumatoid arthritis theranostics. *Sci Rep*. 2015;5:11518.

Publisher's Note

Springer Nature remains neutral with regard to jurisdictional claims in published maps and institutional affiliations.

Ready to submit your research? Choose BMC and benefit from:

- fast, convenient online submission
- thorough peer review by experienced researchers in your field
- rapid publication on acceptance
- support for research data, including large and complex data types
- gold Open Access which fosters wider collaboration and increased citations
- maximum visibility for your research: over 100M website views per year

At BMC, research is always in progress.

Learn more biomedcentral.com/submissions

